Available online at www.sciencedirect.com
SCIENCE DIRECT
Composite Structures 75 (2006) 593–600
COMPOSITE STRUCTURES
www.elsevier.com/locate/compstruct

Natural frequencies of functionally graded plates by a meshless method

A.J.M. Ferreira [a,*], R.C. Batra [b], C.M.C. Roque [a], L.F. Qian [c], R.M.N. Jorge [a]

[a] Departamento de Engenharia Mecânica e Gestão Industrial, Faculdade de Engenharia da Universidade do Porto, Rua Dr. Roberto Frias, 4200-465 Porto, Portugal
[b] Department of Engineering Science and Mechanics, MC 0219, Virginia Polytechnic Institute and State University, Blacksburg, VA 24061, USA
[c] Department of Mechanical Engineering, Nanjing University of Science and Technology, Nanjing, China

Available online 5 June 2006

Abstract

We use the global collocation method, the first and the third-order shear deformation plate theories, the Mori–Tanaka technique to homogenize material properties, and approximate the trial solution with multiquadric radial basis functions to analyze free vibrations of functionally graded plates. Frequencies computed by the present method are found to agree well with those from the analytical solution of Vel and Batra, and the numerical solution of Qian et al. based on the meshless local Petrov–Galerkin formulation.

Keywords: Collocation method; Multiquadrics; Natural frequencies; Functionally graded plates

1. Introduction

Qian et al. [1,2] recently employed the meshless local Petrov–Galerkin method (MLPG) to analyze free and forced vibrations of both homogeneous and functionally graded (FG) thick plates with the higher-order shear and normal deformable plate theory (HOSNDPT) of Batra and Vidoli [3]. Computed frequencies for a simply supported FG plate were found to match well with those obtained from the analytical solution of the three-dimensional (3D) elasticity equations of Vel and Batra [4]. For a simply supported plate, Vel and Batra [4] used the classical plate theory, the first-order shear deformation (FSDT), and the third-order shear deformation (TSDT) approximations [5] for the displacement fields, assumed each displacement component to vary sinusoidally in the x- and the y-directions, and derived an algebraic equation for the frequencies. The assumed forms of displacements satisfy boundary conditions at the plate edges only when they are simply supported.

Here we use the asymmetric collocation method with multiquadrics basis functions, and the FSDT and the TSDT to find natural frequencies of square FG plates of various aspect ratios, and under different boundary conditions at the edges. This method has been employed earlier by Ferreira et al. [6] to study static deformations of FG plates. An advantage of this method over the finite element method (FEM) is that the discretization of the domain into 2D or 3D elements, and the element connectivity are not needed. The present method, like the MLPG method employed by Qian et al. [1,2], requires only coordinates of nodes on the midsurface of the plate. Thus the input required for the present meshless method, and the effort required to prepare the input are considerably less than that needed for the FEM.

Details of the collocation method with multiquadrics and its application to the analysis of plate problems are given in Refs. [6–13].

2. The finite point multiquadric method

Consider the following linear elliptic boundary-value problem defined on a smooth domain Ω:

* Corresponding author. Tel.: +351 22 957 8713; fax: +351 22 953 7352.
E-mail address: ferreira@fe.up.pt (A.J.M. Ferreira).

0263-8223/$ - see front matter © 2006 Elsevier Ltd. All rights reserved.
doi:10.1016/j.compstruct.2006.04.018

$$\begin{aligned} Lu(\mathbf{x}) &= s(\mathbf{x}), \quad \mathbf{x} \in \Omega, \\ Bu(\mathbf{x}) &= f(\mathbf{x}), \quad \mathbf{x} \in \partial\Omega, \end{aligned} \tag{1}$$

where $\partial\Omega$ is the boundary of Ω, L and B are linear differential operators, and s and f are smooth functions defined on Ω and $\partial\Omega$ respectively. We select N_B points ($\mathbf{x}^{(j)}$, $j = 1,\ldots,N_B$) on $\partial\Omega$ and ($N - N_B$) points ($\mathbf{x}^{(j)}$, $j = N_B + 1$, $N_B + 2,\ldots,N$) in the interior of Ω. Let

$$u^h(\mathbf{x}) = \sum_{j=1}^{N} a_j g(||\mathbf{x} - \mathbf{x}^{(j)}||, c) = \sum_{j=1}^{N} a_j g_j(\mathbf{x}), \tag{2}$$

be an approximate solution of the boundary-value problem where $a_1, a_2, \ldots, a_N$ are constants to be determined, $\|\mathbf{x} - \mathbf{x}^{(j)}\|$ is the Euclidean distance between points $\mathbf{x}$ and $\mathbf{x}^{(j)}$, c is a constant, and g is a function of $\|\mathbf{x} - \mathbf{x}^{(j)}\|$ and c. Different forms of functions g and names associated with them are

$$\begin{aligned} &\text{Multiquadrics:} \quad g_j(\mathbf{x}) = (||\mathbf{x} - \mathbf{x}^{(j)}||^2 + c^2)^{1/2}, \\ &\text{Inverse multiquadrics:} \quad g_j(\mathbf{x}) = (||\mathbf{x} - \mathbf{x}^{(j)}||^2 + c^2)^{-1/2}, \\ &\text{Gaussian:} \quad g_j(\mathbf{x}) = \mathrm{e}^{-c^2||\mathbf{x}-\mathbf{x}^{(j)}||^2}, \\ &\text{Thin plate splines:} \quad g_j(\mathbf{x}) = ||\mathbf{x} - \mathbf{x}^{(j)}||^2 \log||\mathbf{x} - \mathbf{x}^{(j)}||. \end{aligned} \tag{3}$$

Substitution from (2) into (1) and evaluating equations resulting from $(1)_2$ at the N_B points $\mathbf{x}^{(j)}$, $j = 1,2,\ldots,N_B$, and from $(1)_1$ at ($N - N_B$) points $\mathbf{x}^{(j)}$, $j = N_B + 1$, $N_B + 2,\ldots,N$ give the following N algebraic equations for the determination of $a_1, a_2, \ldots, a_N$.

$$\begin{aligned} &\sum_{j=1}^{N} a_j Lg(||\mathbf{x} - \mathbf{x}^{(j)}||, c)|_{\mathbf{x}=\mathbf{x}^{(i)}} = s(\mathbf{x}^{(i)}), \\ &\quad i = N_B + 1, N_B + 2, \ldots, N, \\ &\sum_{j=1}^{N} a_j Bg(||\mathbf{x} - \mathbf{x}^{(j)}||, c)|_{\mathbf{x}=\mathbf{x}^{(i)}} = f(\mathbf{x}^{(i)}), \quad i = 1, 2, \ldots, N_B \end{aligned} \tag{4}$$

Depending upon the value of the parameter c and the form of function g, the set of Eq. (4) that determines $a_1, a_2, \ldots, a_N$ may become ill-conditioned; e.g. see [14]. Also, the computational effort involved in solving (4) for $a_1, a_2, \ldots, a_N$ varies with the choice of the function g. Once Eqs. (4) have been solved for a's, then the approximate solution of the problem is given by (2).

3. Review of the third-order shear deformation plate theory

A schematic sketch of the problem studied, dimensions of the FG plate, and the location of the rectangular Cartesian coordinate axes used to describe deformations of the plate are given in Fig. 1. The displacement field in the TSDT is given by

$$u(x,y,z) = u_0(x,y) + z\phi_x - c_1 z^3\left(\phi_x + \frac{\partial w}{\partial x}\right),$$

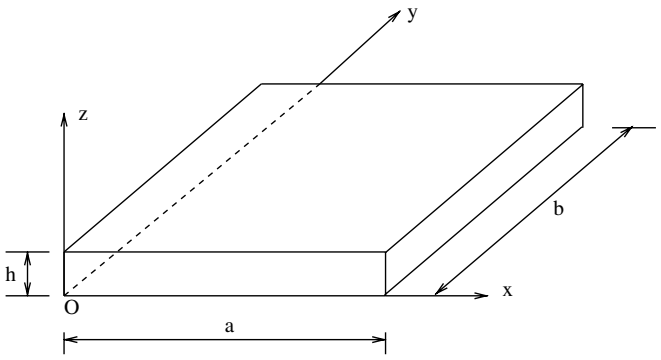

Fig. 1. Plate geometry.

$$\begin{aligned} v(x,y,z) &= v_0(x,y) + z\phi_y - c_1 z^3\left(\phi_y + \frac{\partial w}{\partial y}\right), \\ w(x,y,z) &= w_0(x,y), \end{aligned} \tag{5}$$

where $c_1 = 4/(3h^2)$, h is the plate thickness, z is the coordinate in the thickness direction, the xy-plane of the rectangular Cartesian coordinate system is located in the midplane of the plate. Functions ϕ_x and ϕ_y describe, respectively, rotations about the y- and the x-axes of a line that is along the normal to the midsurface of the plate; u_0, v_0 and w_0 give, respectively, displacements of a point on the midsurface of the plate along the x-, y- and z-axes. The constant c_1 is determined by requiring that the transverse shear strain vanishes on the top and the bottom surfaces of the plate. Note that the transverse normal strain identically vanishes in the TSDT. Batra and Vidoli [3] have proposed a mixed HOSNDPT in which natural boundary conditions prescribed on the top and the bottom surfaces of the plate are exactly satisfied. The displacement field for the FSDT can be obtained from (5) by setting $c_1 = 0$.

From the strain–displacement relations appropriate for infinitesimal deformations, we obtain

$$\begin{Bmatrix} e_{xx} \\ e_{yy} \\ 2e_{xy} \\ 2e_{yz} \\ 2e_{zx} \end{Bmatrix} = \begin{Bmatrix} e_{xx}^{(0)} \\ e_{yy}^{(0)} \\ 2e_{xy}^{(0)} \\ 2e_{yz}^{(0)} \\ 2e_{zx}^{(0)} \end{Bmatrix} + z\begin{Bmatrix} e_{xx}^{(1)} \\ e_{yy}^{(1)} \\ 2e_{xy}^{(1)} \\ 2e_{yz}^{(1)} \\ 2e_{zx}^{(1)} \end{Bmatrix} + z^3\begin{Bmatrix} e_{xx}^{(2)} \\ e_{yy}^{(2)} \\ 2e_{xy}^{(2)} \\ 2e_{yz}^{(2)} \\ 2e_{zx}^{(2)} \end{Bmatrix}, \tag{6}$$

where

$$\begin{Bmatrix} e_{xx}^{(0)} \\ e_{yy}^{(0)} \\ 2e_{xy}^{(0)} \\ 2e_{yz}^{(0)} \\ 2e_{zx}^{(0)} \end{Bmatrix} = \begin{Bmatrix} \dfrac{\partial u_0}{\partial x} \\ \dfrac{\partial v_0}{\partial y} \\ \dfrac{\partial u_0}{\partial y} + \dfrac{\partial v_0}{\partial x} \\ \dfrac{\partial w_0}{\partial y} + \phi_y \\ \dfrac{\partial w_0}{\partial x} + \phi_x \end{Bmatrix},$$

$$\begin{Bmatrix} e_{xx}^{(1)} \\ e_{yy}^{(1)} \\ 2e_{xy}^{(1)} \\ 2e_{yz}^{(1)} \\ 2e_{zx}^{(1)} \end{Bmatrix} = \begin{Bmatrix} \dfrac{\partial \phi_x}{\partial x} \\ \dfrac{\partial \phi_y}{\partial y} \\ \dfrac{\partial \phi_x}{\partial y} + \dfrac{\partial \phi_y}{\partial x} \\ 0 \\ 0 \end{Bmatrix},$$

$$\begin{Bmatrix} e_{xx}^{(2)} \\ e_{yy}^{(2)} \\ 2e_{xy}^{(2)} \\ 2e_{yz}^{(2)} \\ 2e_{zx}^{(2)} \end{Bmatrix} = -c_1 \begin{Bmatrix} \dfrac{\partial \phi_x}{\partial x} + \dfrac{\partial^2 w_0}{\partial x^2} \\ \dfrac{\partial \phi_y}{\partial y} + \dfrac{\partial^2 w_0}{\partial y^2} \\ \dfrac{\partial \phi_x}{\partial y} + \dfrac{\partial \phi_y}{\partial x} + 2\dfrac{\partial^2 w_0}{\partial x \partial y} \\ \dfrac{3}{z}\left(\dfrac{\partial w_0}{\partial y} + \phi_y\right) \\ \dfrac{3}{z}\left(\dfrac{\partial w_0}{\partial x} + \phi_x\right) \end{Bmatrix}. \tag{7}$$

Equations for the plate theory, derived by using the principle of virtual work, are

$$\frac{\partial N_{xx}}{\partial x} + \frac{\partial N_{xy}}{\partial y} = I_0 \frac{\partial^2 u_0}{\partial t^2} + J_1 \frac{\partial^2 \phi_x}{\partial t^2} - c_1 I_3 \frac{\partial^2}{\partial t^2}\left(\frac{\partial w_0}{\partial x}\right), \tag{8}$$

$$\frac{\partial N_{xy}}{\partial x} + \frac{\partial N_{yy}}{\partial y} = I_0 \frac{\partial^2 v_0}{\partial t^2} + J_1 \frac{\partial^2 \phi_y}{\partial t^2} - c_1 I_3 \frac{\partial^2}{\partial t^2}\left(\frac{\partial w_0}{\partial y}\right), \tag{9}$$

$$\begin{aligned} &\frac{\partial \overline{Q}_x}{\partial x} + \frac{\partial \overline{Q}_y}{\partial y} + c_1\left(\frac{\partial^2 P_{xx}}{\partial x^2} + 2\frac{\partial^2 P_{xy}}{\partial x \partial y} + \frac{\partial^2 P_{yy}}{\partial y^2}\right) + q \\ &\quad = I_0 \frac{\partial^2 w_0}{\partial t^2} - c_1 I_6 \frac{\partial^2}{\partial t^2}\left(\frac{\partial^2 w_0}{\partial x^2} + \frac{\partial^2 w_0}{\partial y^2}\right) \\ &\qquad + c_1\left[I_3 \frac{\partial^2}{\partial t^2}\left(\frac{\partial u_0}{\partial x} + \frac{\partial v_0}{\partial y}\right) + J_4 \frac{\partial^2}{\partial t^2}\left(\frac{\partial \phi_x}{\partial x} + \frac{\partial \phi_y}{\partial y}\right)\right], \end{aligned} \tag{10}$$

$$\frac{\partial \overline{M}_{xx}}{\partial x} + \frac{\partial \overline{M}_{xy}}{\partial y} - \overline{Q}_x = \frac{\partial^2}{\partial t^2}\left(J_1 u_0 + K_2 \phi_x - c_1 J_4 \frac{\partial w_0}{\partial x}\right), \tag{11}$$

$$\frac{\partial \overline{M}_{xy}}{\partial x} + \frac{\partial \overline{M}_{yy}}{\partial y} - \overline{Q}_y = \frac{\partial^2}{\partial t^2}\left(J_1 v_0 + K_2 \phi_y - c_1 J_4 \frac{\partial w_0}{\partial y}\right), \tag{12}$$

where q is the sum of the distributed normal tractions applied on the top and the bottom surfaces of the plate, and

$$\overline{M}_{\alpha\beta} = M_{\alpha\beta} - c_1 P_{\alpha\beta}; \quad \overline{Q}_\alpha = Q_\alpha - c_2 R_\alpha, \tag{13}$$

$$\begin{aligned} &I_i = \sum_{k=1}^{N} \int_k^{k+1} \rho^{(k)} (z)^i \, \mathrm{d}z \quad (i = 0, 1, 2, \ldots, 6), \\ &J_i = I_i - c_1 I_{i+2} \quad (i = 1, 4), \\ &K_2 = I_2 - 2c_1 I_4 + c_1^2 I_6, \qquad c_1 = \frac{4}{3h^2}, \quad c_2 = \frac{4}{h^2} = 3c_1, \end{aligned} \tag{14, 15}$$

where α, β take the values x, y. Furthermore (N_{xx}, N_{yy}, N_{xy}) denote the in-plane force resultants, (M_{xx}, M_{yy}, M_{xy}) the moment resultants, (Q_x, Q_y) the shear resultants, and (P_{xx}, P_{yy}, P_{xy}) and (R_x, R_y) the higher-order stress resultants. These are defined by

$$\begin{Bmatrix} N_{\alpha\beta} \\ M_{\alpha\beta} \\ P_{\alpha\beta} \end{Bmatrix} = \int_{-h/2}^{h/2} \sigma_{\alpha\beta} \begin{Bmatrix} 1 \\ z \\ z^3 \end{Bmatrix} \mathrm{d}z, \tag{16}$$

$$\begin{Bmatrix} Q_\alpha \\ R_\alpha \end{Bmatrix} = \int_{-h/2}^{h/2} \sigma_{\alpha z} \begin{Bmatrix} 1 \\ z^2 \end{Bmatrix} \mathrm{d}z. \tag{17}$$

The FSDT equations are readily obtained from those of the TSDT equations by setting $c_1 = 0$.

Expressions for $M_{\alpha\beta}$, $N_{\alpha\beta}$, $P_{\alpha\beta}$, Q_α and R_α in terms of strains can be derived by substituting into (16) and (17) from the following stress–strain relation for an isotropic material:

$$\begin{Bmatrix} \sigma_{xx} \\ \sigma_{yy} \\ \sigma_{xy} \\ \sigma_{yz} \\ \sigma_{zx} \end{Bmatrix} = \begin{bmatrix} Q_{11} & Q_{12} & 0 & 0 & 0 \\ Q_{12} & Q_{11} & 0 & 0 & 0 \\ 0 & 0 & Q_{33} & 0 & 0 \\ 0 & 0 & 0 & kQ_{33} & 0 \\ 0 & 0 & 0 & 0 & kQ_{33} \end{bmatrix} \begin{Bmatrix} e_{xx} \\ e_{yy} \\ 2e_{xy} \\ 2e_{yz} \\ 2e_{zx} \end{Bmatrix}, \tag{18}$$

where

$$\begin{aligned} &Q_{11} = E/(1 - \nu^2), \quad Q_{12} = \nu E/(1 - \nu^2), \\ &Q_{33} = E/2(1 + \nu), \end{aligned} \tag{19}$$

E is the effective Young's modulus, and ν the effective Poisson's ratio at a point in a FG plate. The shear correction factor, k, is taken as 5/6 for the FSDT and 1.0 for the TSDT.

Substitution for strains in terms of displacements from (5) into (6), for stresses from (18) into (16), for $M_{\alpha\beta}$, $N_{\alpha\beta}$, etc. from (16) into (8)–(12) yield equations of motion in terms of the generalized displacements u_0, v_0, w_0,ϕ_x and ϕ_y; these are summarized in Appendix I. An approximate solution of these equations and the pertinent boundary conditions is found by using the meshless method described in Section 2. That is, we assume that

$$u_0^h(\mathbf{x}) = \sum_{j=1}^{N} a_j^u g(||\mathbf{x} - \mathbf{x}^{(j)}||, c), \text{ etc.} \tag{20}$$

These expressions are substituted in equations of motion listed in Appendix I, and also in relevant boundary conditions.

Boundary conditions at a simply supported edge, $x = a$, are

$$\begin{aligned} &w_0(a, y) = 0, \quad v_0(a, y) = 0, \quad \phi_y(a, y) = 0, \\ &N_{xx}(a, y) = 0, \quad \overline{M}_{xx}(a, y) = 0. \end{aligned} \tag{21}$$

Boundary conditions imposed at a rigidly clamped edge, $y = b$, are

$$\begin{aligned} &u_0(x, b) = 0, \quad v_0(x, b) = 0, \quad w_0(x, b) = 0, \\ &\phi_x(x, b) = 0, \quad \phi_y(x, b) = 0. \end{aligned} \tag{22}$$

Boundary conditions imposed at a free edge, $x = a$, are

$$\begin{aligned} &\overline{Q}_x(a, y) = 0, \quad N_{xx}(a, y) = 0, \quad N_{xy}(a, y) = 0, \\ &\overline{M}_{xy}(a, y) = 0, \quad \overline{M}_{xx}(a, y) = 0. \end{aligned} \tag{23}$$

4. Homogenization of material properties

We assume that the plate is made of two randomly distributed isotropic constituents, the macroscopic response of the composite is isotropic, and its composition varies only in the z-direction. Qian and Batra [15] have studied free vibrations of a FG plate with material properties varying smoothly in two directions. The volume fraction of constituent 1 is assumed to be given by

$$V_1 = V_1^- + (V_1^+ - V_1^-)\left(\frac{1}{2} + \frac{z}{h}\right)^p.$$

Thus $V_1 = V_1^-$ at the bottom surface $z = -h/2$, and $V_1 = V_1^+$ at the top surface $z = h/2$ of the plate. Fig. 2 depicts the through-the-thickness distribution of the volume fraction of phase 1 for different values of p.

Here we employ the Mori–Tanaka [16] homogenization method to find the effective bulk modulus, K, and the effective shear modulus, G, of the composite from

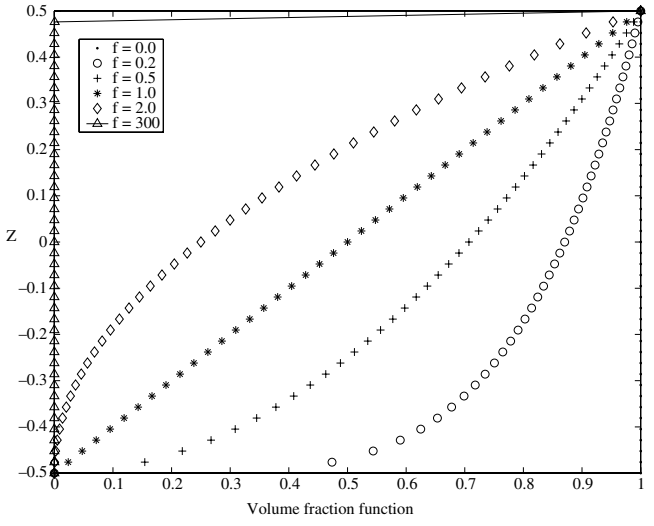

Fig. 2. Through-the-thickness distribution of volume fraction.

Table 1
Fundamental frequency of a simply supported square thick Al/ZrO_2 FG plate, TSDT, $V_c^- = 0$, $V_c^+ = 1$, $p = 1$

$h/a = 0.05$			$h/a = 0.1$			$h/a = 0.2$		
Present	Ref. [2]	Exact	Present	Ref. [2]	Exact	Present	Ref. [2]	Exact
0.0147	0.0149	0.0153	0.0592	0.0584	0.0596	0.2188	0.2152	0.2192

Table 2
Fundamental frequency of a simply supported square thick Al/ZrO_2 FG plate, TSDT, $V_c^- = 0$, $V_c^+ = 1$, $h/a = 0.2$

$p = 2$			$p = 3$			$p = 5$		
Present	Ref. [2]	Exact	Present	Ref. [2]	Exact	Present	Ref. [2]	Exact
0.2188	0.2153	0.2197	0.2202	0.2172	0.2211	0.2215	0.2194	0.2225

Table 3
First 10 natural frequencies of a simply supported square thick Al/ZrO_2 FG plate, TSDT, $V_c^- = 0$, $V_c^+ = 1$, $h/a = 0.2$

Ceramic				$p = 1$				$p = 2$				$p = 5$				Metal			
$N = 7$	$N = 9$	$N = 11$	Ref. [2]	$N = 7$	$N = 9$	$N = 11$	Ref. [2]	$N = 7$	$N = 9$	$N = 11$	Ref. [2]	$N = 7$	$N = 9$	$N = 11$	Ref. [2]	$N = 7$	$N = 9$	$N = 11$	Ref. [2]
0.2468	0.2459	0.2457	0.2469	0.2192	0.2185	0.2188	0.2152	0.2197	0.2190	0.2188	0.2153	0.2224	0.2217	0.2215	0.2194	0.2121	0.2113	0.2111	0.2122
0.4459	0.4474	0.4483	0.4535	0.4047	0.4061	0.3990	0.4114	0.3970	0.3983	0.3991	0.4034	0.3900	0.3914	0.3921	0.3964	0.3831	0.3845	0.3852	0.3897
0.4462	0.4476	0.4484	0.4535	0.4050	0.4062	0.3992	0.4114	0.3972	0.3985	0.3992	0.4034	0.3902	0.3915	0.3922	0.3964	0.3834	0.3846	0.3853	0.3897
0.5409	0.5400	0.5395	0.5441	0.4818	0.4810	0.4779	0.4761	0.4788	0.4783	0.4779	0.4720	0.4800	0.4798	0.4794	0.4760	0.4647	0.4640	0.4636	0.4675
0.5410	0.5401	0.5395	0.5441	0.4818	0.4810	0.4779	0.4761	0.4789	0.4783	0.4779	0.4720	0.4801	0.4798	0.4795	0.4760	0.4648	0.4640	0.4636	0.4675
0.6603	0.6509	0.6470	0.6418	0.5990	0.5906	0.5759	0.5820	0.5876	0.5793	0.5759	0.5709	0.5774	0.5692	0.5658	0.5611	0.5674	0.5593	0.5560	0.5517
0.7843	0.7821	0.7809	0.7881	0.6997	0.6977	0.6897	0.6914	0.6923	0.6906	0.6897	0.6817	0.6907	0.6893	0.6884	0.6832	0.6839	0.6720	0.6710	0.6772
0.8881	0.8963	0.899	0.9076	0.8057	0.8131	0.8001	0.8192	0.7904	0.7977	0.8001	0.8056	0.7767	0.7839	0.7863	0.7928	0.7631	0.7702	0.7725	0.7615
0.8896	0.8970	0.8994	0.9326	0.8070	0.8137	0.8163	0.8217	0.7917	0.7982	0.8004	0.8105	0.7780	0.7844	0.7866	0.8053	0.7644	0.7707	0.7728	0.7799
0.9130	0.9195	0.9209	0.9354	0.8150	0.8208	0.8118	0.8242	0.8040	0.8104	0.8118	0.9022	0.7996	0.8065	0.8081	0.8099	0.7845	0.7901	0.7913	0.8013

$$\frac{K-K_1}{K_2-K_1}=\frac{V_2}{1+(1-V_2)\frac{K_2-K_1}{K_1+\frac{4}{3}G_1}},$$
$$\frac{G-G_1}{G_2-G_1}=\frac{V_2}{1+(1-V_2)\frac{G_2-G_1}{G_1+f_1}}, \tag{24}$$

where $f_1=\frac{G_1(9K_1+8G_1)}{6(K_1+2G_1)}$. The effective values of Young's modulus, E, and Poisson's ratio, v, are found from

$$E=\frac{9KG}{3K+G}, \qquad v=\frac{3K-2G}{2(3K+G)}. \tag{25}$$

5. Results

We compute results for a FG plate comprised of aluminum and zirconia mainly because analytical results for a plate made of these materials are available for comparison [4]. Material properties of the aluminum (Al) and zirconia (ZrO_2) are

$$\text{Al:}\quad E_m=70\text{ GPa},\quad v_m=0.3,\quad \rho_m=2702\text{ kg/m}^3,$$
$$\text{ZrO}_2\text{:}\quad E_z=200\text{ GPa},\quad v_z=0.3,\quad \rho_z=5700\text{ kg/m}^3.$$

We assume that the volume fraction of the ceramic phase is given by (24) and henceforth replace subscripts 1 and 2 by c and m respectively.

Natural frequencies are non-dimensionalized by

$$\bar{\omega}=\omega h\sqrt{\frac{\rho_m}{E_m}}.$$

We consider simply supported (SSSS), clamped (CCCC), simply supported/clamped (SCSC) and clamped/free (CFCF) boundary conditions. Notation SCSC, for example, indicates that edges $x=0$ and $x=a$ are simply supported (S), and edges $y=0$ and $y=b$ are clamped (C).

When possible, we compare present results with existing ones. We use multiquadric functions $(3)_1$ with $c=6d$, d being the distance between two consecutive nodes. For a square plate, we use nodes equally spaced in the x- and the y-directions.

In Tables 1 and 2 the fundamental frequency from the present meshless method, with 11×11 uniformly spaced

Table 4
First 10 natural frequencies of a simply supported square thick FG plate, TSDT, $V_c^-=0$, $V_c^+=1$, $p=1.0$

$h/a=0.05$				$h/a=0.1$			
$N=7$	$N=9$	$N=11$	Ref. [2]	$N=7$	$N=9$	$N=11$	Ref. [2]
0.0147	0.0148	0.0147	0.0149	0.0594	0.0592	0.0592	0.0584
0.0394	0.0381	0.0375	0.0377	0.1450	0.1433	0.1428	0.1410
0.0404	0.0382	0.0375	0.0377	0.1450	0.1433	0.1428	0.1410
0.0679	0.0594	0.0592	0.0593	0.2024	0.2031	0.2035	0.2058
0.0679	0.0754	0.0749	0.0747	0.2025	0.2031	0.2035	0.2058
0.0737	0.0756	0.0753	0.0747	0.2218	0.2193	0.2191	0.2164
0.0884	0.0940	0.0952	0.0769	0.2690	0.2682	0.2678	0.2646
0.0919	0.0991	0.0952	0.0912	0.2794	0.2685	0.2679	0.2677
0.1012	0.1015	0.1017	0.0913	0.2996	0.2954	0.2936	0.2913
0.1013	0.1016	0.1018	0.1029	0.3421	0.3377	0.3363	0.3264

Table 5
First 10 natural frequencies of a simply supported square thick Al/ZrO_2 FG plate, FSDT, $V_c^-=0$, $V_c^+=1$, $h/a=0.2$

Ceramic				$p=1$				$p=2$				$p=5$				Metal			
$N=7$	$N=9$	$N=11$	Ref. [2]	$N=7$	$N=9$	$N=11$	Ref. [2]	$N=7$	$N=9$	$N=11$	Ref. [2]	$N=7$	$N=9$	$N=11$	Ref. [2]	$N=7$	$N=9$	$N=11$	Ref. [2]
0.2479	0.2467	0.2462	0.2469	0.2205	0.2195	0.2191	0.2152	0.2218	0.2207	0.2203	0.2153	0.2251	0.2240	0.2236	0.2194	0.2130	0.212	0.2116	0.2122
0.4459	0.4474	0.4483	0.4535	0.4047	0.4061	0.4069	0.4114	0.3970	0.3983	0.3991	0.4034	0.3900	0.3914	0.3921	0.3964	0.3831	0.3845	0.3852	0.3897
0.4462	0.4476	0.4484	0.4535	0.4049	0.4062	0.4069	0.4114	0.3972	0.3985	0.3992	0.4034	0.3902	0.3915	0.3922	0.3964	0.3834	0.3846	0.3853	0.3897
0.5430	0.5407	0.5397	0.5441	0.4852	0.4831	0.4822	0.4761	0.4853	0.4833	0.4825	0.4720	0.4887	0.4869	0.4861	0.4760	0.4665	0.4646	0.4638	0.4675
0.5431	0.5408	0.5398	0.5441	0.4854	0.4831	0.4822	0.4761	0.4854	0.4834	0.4825	0.4720	0.4888	0.4869	0.4861	0.4760	0.4667	0.4647	0.4638	0.4675
0.6603	0.6509	0.6470	0.6418	0.5991	0.5906	0.5871	0.5820	0.5877	0.5793	0.5759	0.5709	0.5774	0.5693	0.5659	0.5611	0.5674	0.5593	0.5560	0.5517
0.7861	0.7821	0.7804	0.7881	0.7042	0.7004	0.6989	0.6914	0.7023	0.6987	0.6972	0.6817	0.7044	0.7010	0.6995	0.6832	0.6755	0.6720	0.6706	0.6772
0.8881	0.8963	0.8990	0.9076	0.8070	0.8137	0.8159	0.8192	0.7904	0.7976	0.8001	0.8056	0.7767	0.7838	0.7862	0.7928	0.7631	0.7702	0.7725	0.7615
0.8896	0.8970	0.8994	0.9326	0.8070	0.8137	0.8159	0.8217	0.7917	0.7982	0.8004	0.8105	0.7780	0.7844	0.7865	0.8053	0.7644	0.7707	0.7728	0.7799
0.9121	0.9185	0.9198	0.9354	0.8180	0.8236	0.8248	0.8242	0.8145	0.8203	0.8215	0.9022	0.8152	0.8213	0.8226	0.8099	0.7837	0.7892	0.7904	0.8013

Table 6
First 10 natural frequencies of a simply supported square thick Al/ZrO_2 FG plate, FSDT, $V_c^- = 0$, $V_c^+ = 1$, $p = 1.0$

$h/a = 0.05$				$h/a = 0.1$			
$N = 7$	$N = 9$	$N = 11$	Ref. [2]	$N = 7$	$N = 9$	$N = 11$	Ref. [2]
0.0146	0.0148	0.0149	0.0149	0.0594	0.0593	0.0593	0.0584
0.0393	0.0381	0.0378	0.0377	0.1460	0.1437	0.1431	0.1410
0.0393	0.0381	0.0378	0.0377	0.1460	0.1437	0.1431	0.1410
0.0613	0.0598	0.0595	0.0593	0.2024	0.2031	0.2035	0.2058
0.0786	0.0758	0.0749	0.0747	0.2025	0.2031	0.2035	0.2058
0.0789	0.0760	0.0750	0.0747	0.2232	0.2204	0.2196	0.2164
0.1002	0.0967	0.0957	0.0769	0.2696	0.2689	0.2684	0.2646
0.1002	0.0967	0.0957	0.0912	0.2700	0.2691	0.2686	0.2677
0.1012	0.1015	0.1017	0.0913	0.2996	0.2954	0.2936	0.2913
0.1013	0.1016	0.1017	0.1029	0.3444	0.3390	0.3373	0.3264

collocation points (or nodes), is compared with that from the exact solution of Vel and Batra [4], and the meshless Petrov–Galerkin solution of Qian et al. [2]. It is clear that the presently computed first frequency is in excellent agreement with the exact one, particularly for a thick plate. The present method gives closer-to-exact values than Qian et al.'s [2] solution. However in [2] an 8×8 nodal arrangement was used.

In Tables 3–9 we have listed the first ten frequencies computed with the present method by using 7×7, 9×9 and 11×11 collocation points distributed uniformly on the plate's 1×1 midsurface. Whenever possible, we compare results with those of Qian et al. [2].

Table 7
First 10 natural frequencies of a clamped square thick Al/ZrO_2 FG plate, TSDT, $V_c^- = 0$, $V_c^+ = 1$, $h/a = 0.2$

Ceramic			$p = 1$			$p = 2$			$p = 5.0$			Metal		
$N = 7$	$N = 9$	$N = 11$	$N = 7$	$N = 9$	$N = 11$	$N = 7$	$N = 9$	$N = 11$	$N = 7$	$N = 9$	$N = 11$	$N = 7$	$N = 9$	$N = 11$
0.3596	0.3596	0.3598	0.3202	0.3202	0.3204	0.3160	0.3162	0.3165	0.3148	0.3151	0.3154	0.3090	0.3090	0.3092
0.6205	0.6263	0.6282	0.5535	0.5588	0.5605	0.5436	0.5490	0.5507	0.5387	0.5441	0.5458	0.5332	0.5382	0.5398
0.6205	0.6263	0.6282	0.5535	0.5588	0.5605	0.5436	0.5490	0.5507	0.5387	0.5441	0.5458	0.5332	0.5382	0.5398
0.8395	0.8462	0.8486	0.7497	0.7558	0.7579	0.7355	0.7415	0.7435	0.7279	0.7338	0.7358	0.7214	0.7272	0.7291
0.8718	0.8696	0.8687	0.7895	0.7875	0.7867	0.7747	0.7727	0.7719	0.7617	0.7597	0.759	0.7491	0.7472	0.7464
0.8718	0.8696	0.8687	0.7895	0.7875	0.7867	0.7747	0.7727	0.7719	0.7617	0.7597	0.759	0.7491	0.7472	0.7464
0.9441	0.9639	0.9685	0.8427	0.8610	0.8653	0.8257	0.8437	0.8480	0.8163	0.8340	0.8384	0.8112	0.8282	0.8322
0.9543	0.9739	0.9784	0.8519	0.8700	0.8742	0.8341	0.8519	0.8562	0.8239	0.8415	0.8458	0.8200	0.8369	0.8407
1.0293	1.0325	1.0331	0.9334	0.9363	0.9369	0.9158	0.9186	0.9192	0.9000	0.9029	0.9034	0.8844	0.8872	0.8877
1.1313	1.1489	1.1542	1.0113	1.0271	1.0320	0.9898	1.0057	1.0106	0.9771	0.9931	0.9980	0.9721	0.9872	0.9918

Table 8
First 10 natural frequencies of a SCSC thick Al/ZrO_2 FG plate, TSDT, $V_c^- = 0$, $V_c^+ = 1$, $h/a = 0.2$

Ceramic			$p = 1$			$p = 2$			$p = 5.0$			Metal		
$N = 7$	$N = 9$	$N = 11$	$N = 7$	$N = 9$	$N = 11$	$N = 7$	$N = 9$	$N = 11$	$N = 7$	$N = 9$	$N = 11$	$N = 7$	$N = 9$	$N = 11$
0.3070	0.3066	0.3066	0.2732	0.2729	0.2729	0.2708	0.2706	0.2706	0.2709	0.2708	0.2709	0.2638	0.2635	0.2635
0.4495	0.4504	0.4509	0.4079	0.4088	0.4093	0.4001	0.4010	0.4014	0.3931	0.3940	0.3944	0.3862	0.3871	0.3875
0.5581	0.5579	0.5578	0.4973	0.4971	0.4970	0.4928	0.4929	0.4928	0.4927	0.4930	0.4930	0.4796	0.4794	0.4793
0.6004	0.6064	0.6082	0.5355	0.5409	0.5426	0.5269	0.5323	0.5340	0.5231	0.5285	0.5302	0.5159	0.5211	0.5226
0.8023	0.8004	0.7997	0.7221	0.7246	0.7250	0.7113	0.7119	0.7113	0.7013	0.6997	0.6991	0.6894	0.6878	0.6871
0.8090	0.8118	0.8126	0.7273	0.7256	0.7254	0.7136	0.7139	0.7147	0.7067	0.7094	0.7101	0.6951	0.6975	0.6982
0.8627	0.8579	0.8558	0.7811	0.7768	0.7750	0.7665	0.7622	0.7604	0.7537	0.7495	0.7477	0.7413	0.7371	0.7354
0.8946	0.9007	0.9025	0.8115	0.8171	0.8187	0.7961	0.8015	0.8032	0.7824	0.7877	0.7893	0.7687	0.7739	0.7755
0.9133	0.9237	0.9258	0.8151	0.8246	0.8266	0.8045	0.8138	0.8158	0.8005	0.8097	0.8116	0.7848	0.7937	0.7955
0.9410	0.9610	0.9656	0.8402	0.8586	0.8629	0.8236	0.8416	0.8460	0.8144	0.8322	0.8366	0.8085	0.8257	0.8297

Table 9
First 10 natural frequencies of a CFCF thick Al/ZrO_2 FG plate, TSDT, $V_c^- = 0$, $V_c^+ = 1$, $h/a = 0.2$

Ceramic			$p = 1$			$p = 2$			$p = 5.0$			Metal		
$N = 7$	$N = 9$	$N = 11$	$N = 7$	$N = 9$	$N = 11$	$N = 7$	$N = 9$	$N = 11$	$N = 7$	$N = 9$	$N = 11$	$N = 7$	$N = 9$	$N = 11$
0.2434	0.2383	0.2362	0.2162	0.2120	0.2117	0.2140	0.2095	0.2089	0.2130	0.2085	0.2103	0.2083	0.2055	0.2044
0.2738	0.2611	0.2614	0.2438	0.2325	0.2324	0.2381	0.2307	0.2298	0.2362	0.2300	0.2306	0.2345	0.2233	0.2250
0.4197	0.4231	0.4227	0.3802	0.3778	0.3769	0.3734	0.3757	0.3755	0.3669	0.3699	0.3696	0.3606	0.3636	0.3632
0.4275	0.4246	0.4248	0.3806	0.3838	0.3834	0.3776	0.3765	0.3761	0.3782	0.3772	0.3764	0.3667	0.3649	0.3657
0.5183	0.5278	0.5310	0.4618	0.4704	0.4734	0.4541	0.4626	0.4654	0.4508	0.4592	0.4617	0.4453	0.4536	0.4563
0.5448	0.5603	0.5669	0.4855	0.4995	0.5056	0.4786	0.4924	0.4981	0.4763	0.4900	0.4952	0.4682	0.4813	0.4871
0.7306	0.7309	0.7298	0.6513	0.6515	0.6507	0.6437	0.6436	0.6425	0.6415	0.6414	0.6398	0.6279	0.6280	0.6270
0.7340	0.7400	0.7417	0.6624	0.6602	0.6612	0.6526	0.6554	0.6566	0.6420	0.6525	0.6527	0.6307	0.6358	0.6374
0.7428	0.7465	0.7469	0.6652	0.6765	0.6766	0.6573	0.6638	0.6639	0.6575	0.6548	0.6570	0.6383	0.6415	0.6418
0.7525	0.7494	0.7521	0.6814	0.6788	0.6816	0.6687	0.6661	0.6687	0.6575	0.6557	0.6574	0.6466	0.6439	0.6463

For all cases studied, the computed frequencies are found to be close to those given by Qian et al. [2]. Whereas integrals over subdomains of Ω appearing in the MLPG weak formulation need to be evaluated numerically, that is not the case here. Thus the present meshless method is computationally more efficient than the MLPG method.

6. Conclusions

The collocation method with multiquadric radial basis functions to approximate the trial solution and the third-order shear deformation theory are found to give frequencies of functionally graded plates that agree very well with those found by Vel and Batra by solving analytically the three-dimensional elasticity equations. The present method is very efficient since it neither requires nodal connectivity nor evaluation of any integral over a subdomain of plate's midsurface. The accuracy of computed frequencies is controlled by the number of collocation points or nodes, their locations, and the parameter, c, in the multiquadric basis functions.

Acknowledgements

The financial support of the INTERREG programme, through grant MNAA – Materials Network for the Atlantic Arc, is gratefully acknowledged. RCB's work was partially supported by the ONR grant N00014-98-1-0300 to Virginia Polytechnic Institute and State University with Dr. Y.D.S. Rajapakse as the program manager. Views expressed herein are those of authors and not of funding agencies.

Appendix I

Equations for the determination of the generalized displacements u_0, v_0, w_0, ϕ_x and ϕ_y of a TSDT are listed below.

$$
\begin{aligned}
&A_{11}\frac{\partial^2 u_0}{\partial x^2}+A_{12}\frac{\partial^2 v_0}{\partial y\,\partial x}+B_{11}\frac{\partial^2 \phi_x}{\partial x^2}+B_{12}\frac{\partial^2 \phi_y}{\partial y\,\partial x}\\
&\quad-\frac{4}{3h^2}E_{11}\left(\frac{\partial^2 \phi_x}{\partial x^2}+\frac{\partial^3 w_0}{\partial x^3}\right)-\frac{4}{3h^2}E_{12}\left(\frac{\partial^2 \phi_y}{\partial y\,\partial x}+\frac{\partial^3 w_0}{\partial y^2\,\partial x}\right)\\
&\quad+A_{33}\left(\frac{\partial^2 u_0}{\partial y^2}+\frac{\partial^2 v_0}{\partial y\,\partial x}\right)+B_{33}\left(\frac{\partial^2 \phi_x}{\partial y^2}+\frac{\partial^2 \phi_y}{\partial y\,\partial x}\right)\\
&\quad-\frac{4}{3h^2}E_{33}\left(\frac{\partial^2 \phi_x}{\partial y^2}+\frac{\partial^2 \phi_y}{\partial y\,\partial x}+2\frac{\partial^3 w_0}{\partial y^2\,\partial x}\right)\\
&\quad=I_0\frac{\partial^2 u_0}{\partial t^2}+J_1\frac{\partial^2 \phi_x}{\partial t^2}-c_1 I_3\frac{\partial^2}{\partial t^2}\left(\frac{\partial w_0}{\partial x}\right),
\end{aligned}
\tag{A.1}
$$

$$
\begin{aligned}
&A_{33}\left(\frac{\partial^2 u_0}{\partial y\,\partial x}+\frac{\partial^2 v_0}{\partial x^2}\right)+B_{33}\left(\frac{\partial^2 \phi_x}{\partial y\,\partial x}+\frac{\partial^2 \phi_y}{\partial x^2}\right)\\
&\quad-\frac{4}{3h^2}E_{33}\left(\frac{\partial^2 \phi_x}{\partial y\,\partial x}+\frac{\partial^2 \phi_y}{\partial x^2}+2\frac{\partial^3 w_0}{\partial y\,\partial x^2}\right)\\
&\quad+A_{12}\frac{\partial^2 u_0}{\partial y\,\partial x}+A_{22}\frac{\partial^2 v_0}{\partial y^2}+B_{12}\frac{\partial^2 \phi_x}{\partial y\,\partial x}+B_{22}\frac{\partial^2 \phi_y}{\partial y^2}\\
&\quad-\frac{4}{3h^2}E_{12}\left(\frac{\partial^2 \phi_x}{\partial y\,\partial x}+\frac{\partial^3 w_0}{\partial y\,\partial x^2}\right)-\frac{4}{3h^2}E_{22}\left(\frac{\partial^2 \phi_y}{\partial y^2}+\frac{\partial^3 w_0}{\partial y^3}\right)\\
&\quad=I_0\frac{\partial^2 v_0}{\partial t^2}+J_1\frac{\partial^2 \phi_y}{\partial t^2}-c_1 I_3\frac{\partial^2}{\partial t^2}\left(\frac{\partial w_0}{\partial y}\right),
\end{aligned}
\tag{A.2}
$$

$$
\begin{aligned}
&A_{55}\left(\frac{\partial \phi_x}{\partial x}+\frac{\partial^2 w_0}{\partial x^2}\right)-\frac{8}{h^2}D_{55}\left(\frac{\partial \phi_x}{\partial x}+\frac{\partial^2 w_0}{\partial x^2}\right)\\
&\quad+\frac{16}{h^4}F_{55}\left(\frac{\partial \phi_x}{\partial x}+\frac{\partial^2 w_0}{\partial x^2}\right)+A_{44}\left(\frac{\partial \phi_y}{\partial y}+\frac{\partial^2 w_0}{\partial y^2}\right)\\
&\quad-\frac{8}{h^2}D_{44}\left(\frac{\partial \phi_y}{\partial y}+\frac{\partial^2 w_0}{\partial y^2}\right)+\frac{16}{h^4}F_{44}\left(\frac{\partial \phi_y}{\partial y}+\frac{\partial^2 w_0}{\partial y^2}\right)\\
&\quad+\frac{4}{3}\left[E_{11}\frac{\partial^3 u_0}{\partial x^3}+E_{12}\frac{\partial^3 v_0}{\partial y\,\partial x^2}+F_{11}\frac{\partial^3 \phi_x}{\partial x^3}+F_{12}\frac{\partial^3 \phi_y}{\partial y\,\partial x^2}\right.\\
&\quad-\frac{4}{3h^2}H_{11}\left(\frac{\partial^3 \phi_x}{\partial x^3}+\frac{\partial^4 w_0}{\partial x^4}\right)-\frac{4}{3h^2}H_{12}\left(\frac{\partial^3 \phi_y}{\partial y\,\partial x^2}+\frac{\partial^4 w_0}{\partial y^2\,\partial x^2}\right)\\
&\quad+2E_{33}\left(\frac{\partial^3 u_0}{\partial y^2\,\partial x}+\frac{\partial^3 v_0}{\partial y\,\partial x^2}\right)+2F_{33}\left(\frac{\partial^3 \phi_x}{\partial y^2\,\partial x}+\frac{\partial^3 \phi_y}{\partial y\,\partial x^2}\right)\\
&\quad-\frac{8}{3h^2}H_{33}\left(\frac{\partial^3 \phi_x}{\partial y^2\,\partial x}+\frac{\partial^3 \phi_y}{\partial y\,\partial x^2}+2\frac{\partial^4 w_0}{\partial y^2\,\partial x^2}\right)+E_{12}\frac{\partial^3 u_0}{\partial y^2\,\partial x}\\
&\quad+E_{22}\frac{\partial^3 v_0}{\partial y^3}+F_{12}\frac{\partial^3 \phi_x}{\partial y^2\,\partial x}+F_{22}\frac{\partial^3 \phi_y}{\partial y^3}\\
&\quad\left.-\frac{4}{3h^2}H_{12}\left(\frac{\partial^3 \phi_x}{\partial y^2\,\partial x}+\frac{\partial^4 w_0}{\partial y^2\,\partial x^2}\right)-\frac{4}{3h^2}H_{22}\left(\frac{\partial^3 \phi_y}{\partial y^3}+\frac{\partial^4 w_0}{\partial y^4}\right)\right]\frac{1}{h^2}\\
&\quad=I_0\frac{\partial^2 w_0}{\partial t^2}-c_1 I_6\frac{\partial^2}{\partial t^2}\left(\frac{\partial^2 w_0}{\partial x^2}+\frac{\partial^2 w_0}{\partial y^2}\right)\\
&\quad+c_1\left[I_3\frac{\partial^2}{\partial t^2}\left(\frac{\partial u_0}{\partial x}+\frac{\partial v_0}{\partial y}\right)+J_4\frac{\partial^2}{\partial t^2}\left(\frac{\partial \phi_x}{\partial x}+\frac{\partial \phi_y}{\partial y}\right)\right],
\end{aligned}
\tag{A.3}
$$

$$
\begin{aligned}
&-A_{55}\left(\phi_x+\frac{\partial w_0}{\partial x}\right)+\frac{8}{h^2}D_{55}\left(\phi_x+\frac{\partial w_0}{\partial x}\right)-\frac{16}{h^4}F_{55}\left(\phi_x+\frac{\partial w_0}{\partial x}\right)\\
&\quad+B_{11}\frac{\partial^2 u_0}{\partial x^2}+B_{12}\frac{\partial^2 v_0}{\partial y\,\partial x}+D_{11}\frac{\partial^2 \phi_x}{\partial x^2}+D_{12}\frac{\partial^2 \phi_y}{\partial y\,\partial x}\\
&\quad-\frac{4}{3h^2}F_{11}\left(\frac{\partial^2 \phi_x}{\partial x^2}+\frac{\partial^3 w_0}{\partial x^3}\right)-\frac{4}{3h^2}F_{12}\left(\frac{\partial^2 \phi_y}{\partial y\,\partial x}+\frac{\partial^3 w_0}{\partial y^2\,\partial x}\right)\\
&\quad-\frac{4}{3}\left[E_{11}\frac{\partial^2 u_0}{\partial x^2}+E_{12}\frac{\partial^2 v_0}{\partial y\,\partial x}+F_{11}\frac{\partial^2 \phi_x}{\partial x^2}+F_{12}\frac{\partial^2 \phi_y}{\partial y\,\partial x}\right.\\
&\quad\left.-\frac{4}{3h^2}H_{11}\left(\frac{\partial^2 \phi_x}{\partial x^2}+\frac{\partial^3 w_0}{\partial x^3}\right)-\frac{4}{3h^2}H_{12}\left(\frac{\partial^2 \phi_y}{\partial y\,\partial x}+\frac{\partial^3 w_0}{\partial y^2\,\partial x}\right)\right]\frac{1}{h^2}
\end{aligned}
$$

$$
\begin{aligned}
&+B_{33}\left(\frac{\partial^2 u_0}{\partial y^2}+\frac{\partial^2 v_0}{\partial y\partial x}\right)+D_{33}\left(\frac{\partial^2 \phi_x}{\partial y^2}+\frac{\partial^2 \phi_y}{\partial y\partial x}\right)\\
&-\frac{4}{3h^2}F_{33}\left(\frac{\partial^2 \phi_x}{\partial y^2}+\frac{\partial^2 \phi_y}{\partial y\partial x}+2\frac{\partial^3 w_0}{\partial y^2\partial x}\right)\\
&-\frac{4}{3}\left[B_{33}\left(\frac{\partial^2 u_0}{\partial y^2}+\frac{\partial v_0}{\partial y\partial x}\right)+F_{33}\left(\frac{\partial^2 \phi_x}{\partial y^2}+\frac{\partial^2 \phi_y}{\partial y\partial x}\right)\right.\\
&\left.-\frac{4}{3h^2}H_{33}\left(\frac{\partial^2 \phi_x}{\partial y^2}+\frac{\partial^2 \phi_y}{\partial y\partial x}+2\frac{\partial^3 w_0}{\partial y^2\partial x}\right)\right]\frac{1}{h^2}\\
&=\frac{\partial^2}{\partial t^2}\left(J_1u_0+K_2\phi_x-c_1J_4\frac{\partial w_0}{\partial x}\right),
\end{aligned}
\tag{A.4}
$$

$$
\begin{aligned}
&-A_{44}\left(\phi_y+\frac{\partial w_0}{\partial y}\right)+\frac{8}{h^2}D_{44}\left(\phi_y+\frac{\partial w_0}{\partial y}\right)-\frac{16}{h^4}F_{44}\left(\phi_y+\frac{\partial w_0}{\partial y}\right)\\
&+B_{12}\frac{\partial^2 u_0}{\partial y\partial x}+B_{22}\frac{\partial^2 v_0}{\partial y^2}+D_{12}\frac{\partial^2 \phi_x}{\partial y\partial x}+D_{22}\frac{\partial^2 \phi_y}{\partial y^2}\\
&-\frac{4}{3h^2}F_{12}\left(\frac{\partial^2 \phi_x}{\partial y\partial x}+\frac{\partial^3 w_0}{\partial y\partial x^2}\right)-\frac{4}{3h^2}F_{22}\left(\frac{\partial^2 \phi_y}{\partial y^2}+\frac{\partial^3 w_0}{\partial y^3}\right)\\
&-\frac{4}{3}\left[E_{12}\frac{\partial^2 u_0}{\partial y\partial x}+E_{22}\frac{\partial^2 v_0}{\partial y^2}+F_{12}\frac{\partial^2 \phi_x}{\partial y\partial x}+F_{22}\frac{\partial^2 \phi_y}{\partial y^2}\right.\\
&\left.-\frac{4}{3h^2}H_{12}\left(\frac{\partial^2 \phi_x}{\partial y\partial x}+\frac{\partial^3 w_0}{\partial y\partial x^2}\right)-\frac{4}{3h^2}H_{22}\left(\frac{\partial^2 \phi_y}{\partial y^2}+\frac{\partial^3 w_0}{\partial y^3}\right)\right]\frac{1}{h^2}\\
&+B_{33}\left(\frac{\partial^2 u_0}{\partial y\partial x}+\frac{\partial^2 v_0}{\partial x^2}\right)+D_{33}\left(\frac{\partial^2 \phi_x}{\partial y\partial x}+\frac{\partial^2 \phi_y}{\partial x^2}\right)\\
&-\frac{4}{3h^2}F_{33}\left(\frac{\partial^2 \phi_x}{\partial y\partial x}+\frac{\partial^2 \phi_y}{\partial x^2}+2\frac{\partial^3 w_0}{\partial y\partial x^2}\right)\\
&-\frac{4}{3}\left[E_{33}\left(\frac{\partial^2 u_0}{\partial y\partial x}+\frac{\partial^2 v_0}{\partial x^2}\right)+F_{33}\left(\frac{\partial^2 \phi_x}{\partial y\partial x}+\frac{\partial^2 \phi_y}{\partial x^2}\right)\right.\\
&\left.-\frac{4}{3h^2}H_{33}\left(\frac{\partial^2 \phi_x}{\partial y\partial x}+\frac{\partial^2 \phi_y}{\partial x^2}+2\frac{\partial^3 w_0}{\partial y\partial x^2}\right)\right]\frac{1}{h^2}\\
&=\frac{\partial^2}{\partial t^2}\left(J_1v_0+K_2\phi_y-c_1J_4\frac{\partial w_0}{\partial y}\right),
\end{aligned}
\tag{A.5}
$$

where

$$
\begin{aligned}
&\left(A_{ij},B_{ij},D_{ij},E_{ij},F_{ij},H_{ij}\right)\\
&=\int_{-\frac{h}{2}}^{\frac{h}{2}}\left((P_t-P_b)\left(\frac{z}{h}+\frac{1}{2}\right)^p(1,z,z^2,z^3,z^4,z^6)\right.\\
&\left.+Q_b(1,z,z^2,z^3,z^4,z^6)\right)\mathrm{d}z
\end{aligned}
\tag{A.6}
$$

where P_t and P_b correspond to generic property at top and bottom surfaces and Q_b correspond to the elasticity matrix at the bottom surface.

References

[1] Qian LF, Batra RC, Chen LM. Free and forced vibrations of thick rectangular plates by using higher-order shear and normal deformable plate theory and meshless local Petrov–Galerkin (MLPG) method. Comput Model Eng Sci 2003;4:519–34.

[2] Qian LF, Batra RC, Chen LM. Static and dynamic deformations of thick functionally graded elastic plate by using higher-order shear and normal deformable plate theory and meshless local Petrov–Galerkin method. Composites: Part B 2004;35:685–97.

[3] Batra RC, Vidoli S. Higher order piezoelectric plate theory derived from a three-dimensional variational principle. AIAA J 2002;40(1): 91–104.

[4] Vel SS, Batra RC. Three-dimensional exact solution for the vibration of functionally graded rectangular plates. J. Sound Vibr 2004; 272:703–30.

[5] Reddy JN. Mechanics of laminated composite plates. New York: CRC Press; 1997.

[6] Ferreira AJM, Batra RC, Roque CMC, Qian LF, Martins PALS. Static analysis of functionally graded plates using third-order shear deformation theory and a meshless method. Comp Struct 2005; 69:449–57.

[7] Hardy RL. Multiquadric equations of topography and other irregular surfaces. Geophys Res 1971;176:1905–15.

[8] Kansa EJ. Multiquadrics – a scattered data approximation scheme with applications to computational fluid dynamics. i. Surface approximations and partial derivative estimates. Comput Math Appl 1990;19(8/9):127–45.

[9] Kansa EJ. Multiquadrics – a scattered data approximation scheme with applications to computational fluid dynamics. ii. Solutions to parabolic, hyperbolic and elliptic partial differential equations. Comput Math Appl 1990;19(8/9):147–61.

[10] Ferreira AJM. A formulation of the multiquadric radial basis function method for the analysis of laminated composite plates. Comp Struct 2003;59:385–92.

[11] Ferreira AJM. Thick composite beam analysis using a global meshless approximation based on radial basis functions. Mech Adv Mater Struct 2003;10:271–84.

[12] Ferreira AJM. Analysis of composite plates using a layerwise shear deformation theory and multiquadrics discretization. Mech Adv Mater Struct 2005;12(2):99–112.

[13] Ferreira AJM, Roque CMC, Martins PALS. Radial basis functions and higher-order theories in the analysis of laminated composite beams and plates. Comp Struct 2004;66:287–93.

[14] Liu GR. Meshfree methods, moving beyond the finite element method. CRC Press; 2002.

[15] Qian LF, Batra RC. Design of bidirectional functionally graded plate for optimal natural frequencies. J Sound Vibr 2005;280:415–24.

[16] Mori T, Tanaka K. Average stress in matrix and average elastic energy of materials with misfitting inclusions. Acta Metall 1973;21:571–4.